ELSEVIER

Journal of Alloys and Compounds 434–435 (2007) 701–703

Journal of ALLOYS AND COMPOUNDS

www.elsevier.com/locate/jallcom

Preparation of molybdenum oxide thin films by MOCVD

R. Martinez Guerrero[a], J.R. Vargas Garcia[a,*], V. Santes[b], E. Gomez[c]

[a] *Depto. de Ingenieria Metalurgica, ESIQIE-IPN, Mexico 07300, D.F., Mexico*
[b] *CIIEMAD-IPN, Miguel Othón de Mendizábal 485, México 07700, D.F., Mexico*
[c] *Instituto de Quimica-UNAM, Circuito Exterior-Ciudad Universitaria, Mexico 04510, D.F., Mexico*

Abstract

In this study, molybdenum oxide films were prepared in a horizontal hot-wall MOCVD apparatus using molybdenum dioxide acetylacetonate as precursor. The molybdenum precursor was synthesized from acetylacetone and molybdenum oxide powder. Thermal gravimetric (TG) and differential thermal analyses (DTA) of the precursor suggested the formation of molybdenum oxides around 430 °C (703 K). Thus, a range of deposition temperatures varying from 350 to 630 °C (623–903 K) was explored to investigate the effects on the nature of the molybdenum oxide films. X-ray diffraction (XRD) results showed that the films consisted of α-MoO_3 phase at deposition temperatures ranging from 400 to 560 °C (673–833 K). Crystalline α-MoO_3 films can be obtained from molybdenum dioxide acetylacetonate precursor, without need of a post-annealing treatment. The best crystalline quality was found in films having needle-like crystallites grown at deposition temperature of about 560 °C (833 K), which exhibit a strong (0 1 0) preferred orientation and a transparent visual appearance.

Keywords: Thin films; Vapour deposition; X-ray diffraction; Thermal analysis

1. Introduction

Molybdenum oxides have become of great technological interest because of their attractive optical, electrochromic and catalytic properties [1–5]. Molybdenum oxide films exhibiting a variety in crystalline phases and surface morphologies are desirables depending on the particular application. Molybdenum oxide deposits combining different crystalline phases and high surface area are important in selective oxidation of methanol and ethanol [6]. In contrast, transparent, amorphous or crystalline MoO_3 films are required in electrochromic devices [7,8]. So far, many methods to prepare molybdenum oxide films have been explored including, thermal evaporation [9], RF sputtering [10], electron beam evaporation [11] and metal organic chemical vapour deposition (MOCVD) [12]. Usually, the synthesis of molybdenum oxide films requires a post-annealing treatment to reach a crystalline state. MOCVD, in particular, is an attractive technique for device integration because of its excellent conformal coverage and low deposition temperatures. Additionally, MOCVD allows for a wide variety in morphologies and crystalline qualities of films by controlling deposition conditions. In this study, we report the preparation by MOCVD of transparent and well crystallized α-MoO_3 films without need of a post-annealing treatment using the molybdenum dioxide acetylacetonate precursor.

2. Experimental

2.1. Synthesis of precursor

Molybdenum precursor for MOCVD experiments was synthesized from MoO_3 powder (Fluka chemika) and acetylacetone (Aldrich). First, 50 ml (5×10^{-4} m^3) of acetylacetone were added to 10 g (1×10^{-2} kg) of MoO_3 powder to react under reflux for 30 h (108 ks). The resulting solution was added to 250 ml (2.5×10^{-3} m^3) of toluene at room temperature for the precipitation of unreacted MoO_3, which was separated by filtering the solution. Then, the solution was heated under nitrogen atmosphere leading to the evaporation of toluene and the precipitation of molybdenum dioxide acetylacetonate ($MoO_2(CH_2COCH_2COCH)_2$); [$MoO_2(acac)_2$ for short]. The red brown product was analyzed by IR and ^{1}H NMR techniques to confirm the formation of $MoO_2(acac)_2$.

2.2. Preparation of films

The molybdenum oxide films were prepared on amorphous glass substrates by decomposition of $MoO_2(acac)_2$ precursor in a horizontal hot-wall MOCVD reactor. The precursor was evaporated at 200 °C (473 K) and its vapours were carrier into to the reactor by nitrogen gas using a gas flow rate of about 100 sccm

---

[*] Corresponding author. Tel.: +52 55 5729 6000x55270; fax: +52 55 5729 6000x55270.
E-mail address: rvargasga@ipn.mx (J.R.V. Garcia).

0925-8388/$ – see front matter © 2006 Elsevier B.V. All rights reserved.
doi:10.1016/j.jallcom.2006.08.227

(1.6×10^{-6} m^3/s). The deposition temperature (T_{dep}) was explored from 350 to 630 °C (623–903 K) and the total pressure (P_{tot}) was kept constant at 1 Torr (133.32 Pa). The deposition time was fixed at 30 min (1.8 ks). A Jeol JSM-6300 scanning electron microscope (SEM) was used to observe the surface morphology. The crystal structure was investigated by X-ray diffraction (XRD) using a Siemens diffractometer (model D5000) with Cu Kα radiation. Thermal gravimetry (TG) and differential thermal analyses (DTA) of the $MoO_2(acac)_2$ were carried out in a SETARAM (model SETSYS12). The IR spectrum was recorded on a Nicolet FT-1 Magna 750 Fourier Transform instrument using pressed disks of mixed KBr and $MoO_2(acac)_2$ powders. The ^1H NMR spectrum was recorded on a Jeol Eclipse +300, in which chemical shifts (ppm) were relative to the TMS.

3. Results and discussion

The IR spectrum for the synthesized $MoO_2(acac)_2$ (not shown here) displayed two significant bands at 918 and 946 cm^{-1} (9.18–9.46 m^{-1}) corresponding to the characteristic stretching vibrations of the cis-MoO_2 arrangement. Additionally, the ^1H NMR spectrum exhibited singlets at 2.12 and 2.14δ assignable to the two sets of inequivalent methyl groups in the molecule of $MoO_2(acac)_2$ [13]. Fig. 1 shows the TG and DTA curves for the $MoO_2(acac)_2$ precursor. The TG curve (dashed line) indicates three different stages of mass change as a function of temperature. The first stage, below 190 °C (463 K), was attributed to the loss of adsorbed water and remained organic solvent. The exothermic peak at about 185 °C (458 K) may arise from the competition between exothermic and endothermic processes related to the evaporation and combustion of the toluene used in the precursor synthesis. The second stage between 190 and 370 °C (463–643 K) was assigned to the decomposition of $MoO_2(acac)_2$ molecule releasing gaseous C–H–O organic compounds consistently with endothermic peak of the DTA curve. At higher temperatures, a third stage of mass stability suggests no decomposition with loss of volatile products, but an oxidation process supported by the DTA exothermic peak at about 430 °C (703 K). As the formation of molybdenum oxides takes place as a gradual process covering a range of temperatures, centered around 430 °C (703 K), the deposition temperature for obtaining oxide films was explored from 350 to 630 °C (623–903 K).

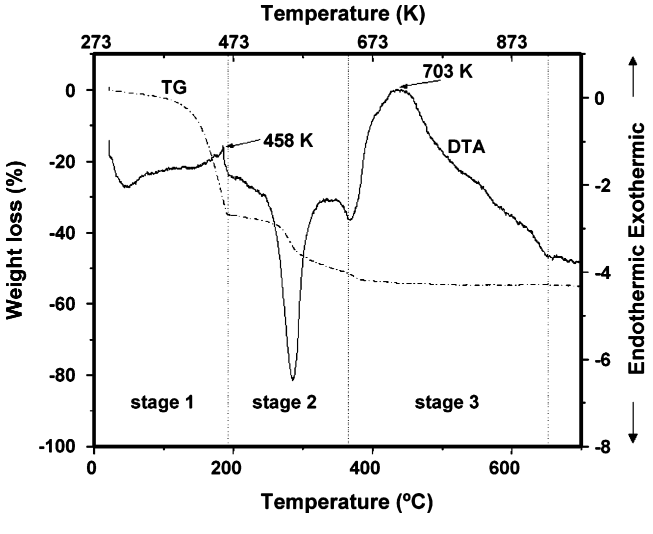

Fig. 1. TG and DTA curves of the synthesized $MoO_2(acac)_2$ precursor.

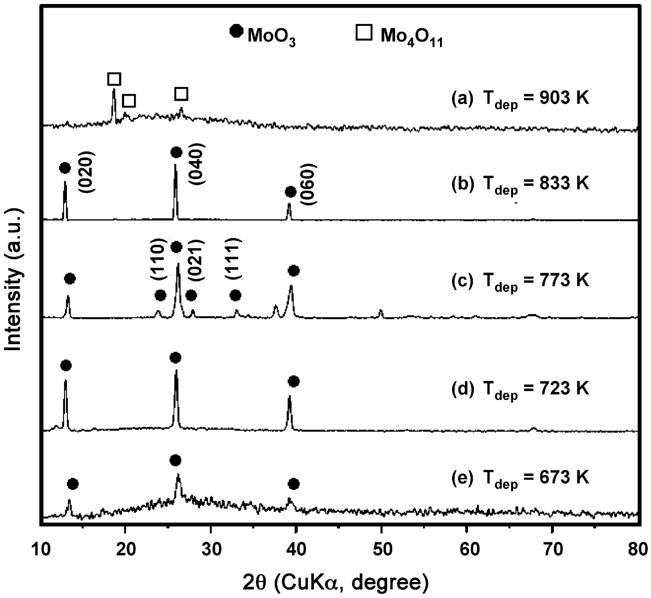

Fig. 2. XRD patterns of molybdenum oxide films prepared at different deposition temperatures.

Fig. 2 depicts the XRD patterns of films prepared at T_{dep} from 400 to 560 °C (673–833 K). Films were obtained from 350 °C (623 K), however, no observable XRD characteristic lines were displayed, suggesting the formation of amorphous and/or very thin films. Nevertheless, films prepared at T_{dep} = 400 °C (673 K) exhibited low intensity XRD lines at $2\theta = 12.6°$, 25.8° and 39.1° corresponding to the (0 2 0), (0 4 0) and (0 6 0) planes of the α-MoO_3 phase according to the JCPDF 5-508 card. This implies that films exhibit a strong (0 1 0) preferred orientation. Further increase in deposition temperature up to 560 °C (833 K), gave rise to well-defined XRD α-MoO_3 lines. Films prepared at T_{dep} = 500 °C (773 K), in particular, showed a polycrystalline nature of the α-MoO_3 films since additional XRD lines belonging to different ($h\,k\,l$) planes of the α-MoO_3 phase appear along with those of ($0\,k\,0$) planes. Higher deposition temperature; T_{dep} = 630 °C (903 K), led to the formation of different oxide phase such as Mo_4O_{11}. No films were obtained at higher temperatures, probably to the evaporation of the MoO_3 phase because of its high vapour pressure at low temperatures. Thus, XRD results demonstrate that α-MoO_3 is the stable phase directly obtained in the as-deposited condition from $MoO_2(acac)_2$ precursor at T_{dep} = 400–560 °C (673–833 K). These results are consistent with the oxidation process suggested by TG and DTA curves in the temperature range of 400–650 °C (673–923 K). In addition, it was observed that appearance and color of films strongly depended on substrate temperature, changing from bluish color at T_{dep} = 400 °C (673 K) to completely transparent at T_{dep} = 560 °C (833 K).

The SEM images, in Fig. 3, illustrate the influence of the deposition temperature on surface morphology and crystallite size of molybdenum oxide films prepared on amorphous glass substrates. The coarse needle-like crystallites (2–4 μm in diameter) observed in Fig. 3a (T_{dep} = 400 °C (673 K)) contrast with the quasi-spherical crystallites (∼1 μm in diameter) in Fig. 3b; T_{dep} = 500 °C (773 K). Additionally, there is an obvious change

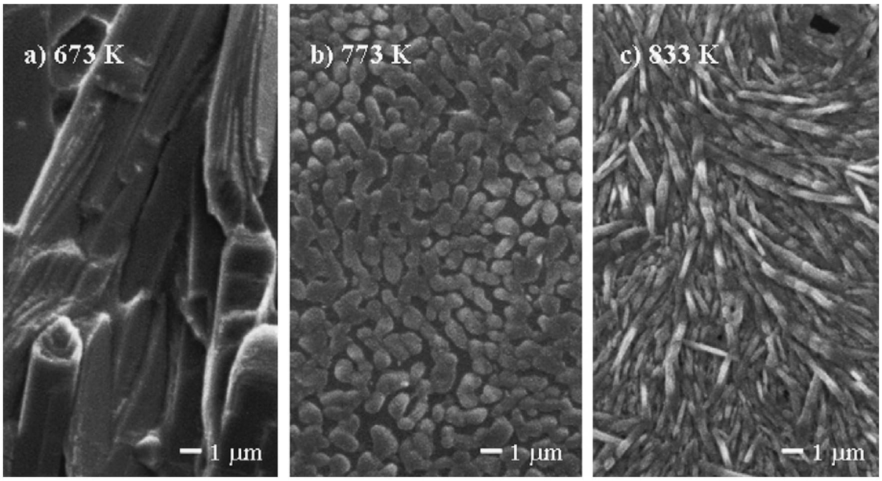

Fig. 3. SEM images of the surface morphology of α-MoO_3 films as a function of the deposition temperature. (a) 400 °C (673 K), (b) 500 °C (773 K) and (c) 560 °C (833 K).

to the needle-like shape again at $T_{dep} = 560\,°C$ (833 K). These needle-like crystallites show a smaller size, less of 1 μm in diameter. Previous reports indicate that films consisting of MoO_3 crystallites exhibit typically needle-like, flake-like or quasi-spherical shapes depending on the annealing temperature, usually 200–600 °C (473–873 K) [7,8,12]. In this study the surface morphology change was attributed to the differences in MoO_3 crystallites orientation forming the films; that is, films prepared at $T_{dep} = 400$ (673), 450 (723) and 560 °C (833 K) have needle-like crystallites that show markedly (0 1 0) preferred orientation, on the other hand, films prepared at $T_{dep} = 500\,°C$ (773 K) exhibit quasi-spherical crystallites of random orientation. Differences in crystalline orientation could be associated with different deposition rates, which mainly depend on deposition temperature and precursor concentration [14]. As deposition temperature was carefully controlled, it follows that precursor concentration might be changed probably to slightly differences in the experimental setting.

4. Conclusions

In this work, it has been demonstrated that uniform and well crystallized α-MoO_3 thin films can be grown by MOCVD on amorphous glass substrates without the need of a post-annealing treatment using the $MoO_2(acac)_2$ precursor. In particular, films grown at $T_{dep} = 560\,°C$ (833 K) exhibit the best crystalline quality with (0 1 0) preferred orientation and a transparent visual appearance. This type of films has promising features to be applied in electrochromic devices.

Acknowledgements

This study was supported by the National Polytechnic Institute (IPN) of Mexico through the project IPN-CGPI: 20051130. One the authors (R. Martinez Guerrero) would like to acknowledge the financial support from IPN and CONACYT through the scholarships for doctor degree studies.

References

[1] S.I. Cordoba de Torresi, A. Gorenstein, R.M. Torresi, M.V. Vazquez, J. Electroanal. Chem. 318 (1991) 131.
[2] M. Klisch, J. Sol-Gel Sci. Technol. 12 (1998) 21.
[3] W. Estrada, A.M. Andersson, C.G. Granqqvist, J. Mater. Res. 1715 (1991) 1715.
[4] S. Jiebing, X. Rui, W. Shimin, T. Wufeng, T. Hua, S. Jing, J. Sol-Gel Sci. Technol. 27 (2003) 315–319.
[5] C.M. Lampert, Solar Energy Mater. 11 (1984) 1.
[6] R.K. Grasselli, J.D. Burrington, Adv. Catat. 30 (1981) 133.
[7] Y.X. Li, K. Galatsis, W. Wlodarski, M. Passacantando, S. Santucci, P. Siciliano, M. Catalano, Sensor Actuator B77 (2001) 27–34.
[8] J. Scarminio, A. Lourenco, A. Gorenstein, Thin Solid Films 302 (1997) 66–70.
[9] S.K. Deb, J.A. Chopoorian, J. Appl. Phys. 37 (1963) 4818.
[10] S.H. Mohamed, O. Kappertz, J.M. Ngaruiya, T.P. Leervad Pedersen, R. Drese, M. Wuttig, Thin Solid Films 429 (2002) 135–143.
[11] M. Yahaya, M.M. Salleh, I.A. Talib, Solid-State Ionics 421 (1998) 113–115.
[12] K.A. Gesheva, A. Szekeres, T. Ivanova, Solar Energy Mater. 76 (2003) 563.
[13] F.J. Arnaiz, J. Chem. Educ. 72 (1995) A7–A8.
[14] T. Kodas, M. Hampden-Smith, The Chemistry of Metal CVD, VCH, Weinheim, 1994.